



Quantitative assessment of muscle mass and gene expression analysis in dogs with glucocorticoid-induced muscle atrophy

Kei YOSHIDA¹⁾, Toshio MATSUOKA^{2,3)}, Yui KOBATAKE²⁾, Satoshi TAKASHIMA²⁾ and Naohito NISHII^{1,2)*}

¹⁾Joint Graduate School of Veterinary Sciences, Gifu University, 1-1 Yanagido, Gifu 501-1193, Japan

²⁾Joint Department of Veterinary Medicine, Faculty of Applied Biological Science, Gifu University, 1-1 Yanagido, Gifu 501-1193, Japan

³⁾Blanco Animal Hospital, Tachibana 3-50, Tsushima, Aichi 496-0038, Japan

ABSTRACT. The present study aimed to quantitatively evaluate muscle mass and gene expression in dogs with glucocorticoid-induced muscle atrophy. Five healthy beagles received oral prednisolone for 4 weeks (1 mg/kg/day), and muscle mass was then evaluated via computed tomography. Histological and gene expression analyses were performed using biopsy samples from the biceps femoris before and after prednisolone administration. The cross-sectional area of the third lumbar paraspinal and mid-femoral muscles significantly decreased after glucocorticoid administration (from 27.5 ± 1.9 to 22.6 ± 2.0 cm² and from 55.1 ± 4.7 to 50.7 ± 4.1 cm², respectively; $P < 0.01$). The fast- and slow-twitch muscle fibers were both atrophied (from $2,779 \pm 369$ to $1,581 \pm 207$ μm² and from $2,871 \pm 211$ to $1,971 \pm 169$ μm², respectively; $P < 0.05$). The expression of the growth factor receptor-bound protein 10 (*GRB10*) significantly increased after prednisolone administration ($P < 0.05$). Because *GRB10* suppresses insulin signaling and the subsequent mammalian target of rapamycin complex 1 activity, increased expression of *GRB10* may have resulted in a decrease in protein anabolism. Taken together, 1 mg/kg/day oral prednisolone for 4 weeks induced significant muscle atrophy in dogs, and *GRB10* might participate in the pathology of glucocorticoid-induced muscle atrophy in canines.

KEY WORDS: dog, glucocorticoids, hyperadrenocorticism, muscle atrophy

J. Vet. Med. Sci.

84(2): 275–281, 2022

doi: 10.1292/jvms.21-0325

Received: 6 June 2021

Accepted: 13 December 2021

Advanced Epub:

3 January 2022

In veterinary medicine, glucocorticoids (GCs) are frequently used for their anti-inflammatory and immunosuppressive effects. Most inflammatory or immune-mediated diseases are refractory; therefore, GCs are often administered for a long term or at high doses. However, long-term or high-dose GC use can cause serious adverse reactions [28]. In dogs, polyuria/polydipsia, glucose intolerance, hepatic or gastrointestinal disorders, and skeletal muscle atrophy are known as the adverse reactions of GC treatment [2]. In particular, skeletal muscle atrophy leads to limb weakness and worsening quality of life [19, 33, 42–44]. Skeletal muscle atrophy is also a problem in dogs with hyperadrenocorticism, which is caused by the excess secretion of endogenous GCs [40]. GC-induced muscle atrophy in canines causes exercise intolerance as well as joint disorders [19, 33, 42–44]; however, GC-induced muscle atrophy is not the direct target of medical intervention. Therefore, no treatment other than reducing GC dose exists both for humans and dogs [36, 37]. Branched chain amino acids, growth hormone, creatine, taurine, and clenbuterol are listed as candidates for treating GC-induced muscle atrophy in humans [21, 28, 37]; however, the efficacy of these candidate treatments has not been established yet.

The mechanism of GC-induced muscle atrophy has not been fully understood. However, GC-induced muscle atrophy has been shown to be triggered by various biological responses, including the inhibition of protein anabolism and promotion of protein catabolism [24, 27, 46]. In rodents, several GC-responsive genes have been implicated in these metabolic abnormalities [3, 39, 46]. These genes can be a promising target in the treatment of GC-induced muscle atrophy. Although GC-induced muscle atrophy is empirically recognized in dogs, there are no reports that have quantitatively proved that GC administration induces muscle atrophy. Furthermore, at present, no study has investigated the molecular biological pathology of GC-induced skeletal muscle atrophy in canines. The pathophysiology of GC-induced muscle atrophy needs clarification for developing appropriate treatment methods. Thus, the present study aimed to elucidate the pathophysiology of GC-induced muscle atrophy in dogs. We induced muscle atrophy

*Correspondence to: Nishii, N.: nishii@gifu-u.ac.jp

(Supplementary material: refer to PMC <https://www.ncbi.nlm.nih.gov/pmc/journals/2350/>)

©2022 The Japanese Society of Veterinary Science



This is an open-access article distributed under the terms of the Creative Commons Attribution Non-Commercial No Derivatives (by-nc-nd) License. (CC-BY-NC-ND 4.0: <https://creativecommons.org/licenses/by-nc-nd/4.0/>)

via GC administration and quantitatively evaluated muscle mass in dogs. Moreover, the expression of 12 genes involved in protein anabolism or catabolism in humans and rodents [3, 10, 12, 17, 20, 31, 32, 35, 45, 47, 48] was analyzed in dogs with GC-induced muscle atrophy.

MATERIALS AND METHODS

Animals and study procedure

Five healthy beagle dogs (two castrated males and three spayed females), with a median weight of 13.7 kg (range 12.5–19.1 kg) and a median age of 5 years (range 4–10 years), were used in this study. The dogs were housed in individual cages under the 12-hr light cycle at approximately 24°C. They were fed commercial maintenance dry food twice a day and allowed free access to tap water. Prednisolone (Predonine tablets 5 mg; Shionogi & Co., Ltd., Osaka, Japan) was administered orally at a dosage of 1 mg/kg body weight once daily for 4 weeks with food. Computed tomography (CT) and muscle biopsy were performed before and after 4 weeks of prednisolone administration. All study procedures were performed in accordance with the Gifu University Guidelines for Animal Experimentation (approval number: 16092).

Evaluation of skeletal muscle mass using CT

We evaluated the skeletal muscle cross-sectional area using CT before and after GC administration for 4 weeks. After 12-hr fasting, the dogs were anesthetized with 7 mg/kg intravenous propofol (PropoFlo; Zoetis Japan, Tokyo, Japan) and maintained with isoflurane (IsoFlo; Zoetis Japan) in oxygen. All CT scans were performed using a multidetector-row CT scanner (Asteion Super 4; Toshiba Medical Systems, Tochigi, Japan) at 120 kV, 100 mA, and 2-mm slice thickness. In humans, the cross-sectional area of the paraspinal muscle at the third lumbar (L3) vertebra correlates with the entire body muscle mass [13, 15]. In addition, the muscles of the proximal lower limbs, including the thigh muscles, are strongly affected in GC-induced muscle atrophy [25]. Therefore, we focused on the paraspinal muscle at L3 and the mid-femoral muscle. The skeletal muscle cross-sectional areas were analyzed using the region of interest tool of OsiriX image software (Newton Graphics, Sapporo, Japan).

Skeletal muscle sampling

After the first CT scan (before GC administration), a skeletal muscle sample was acquired from the left biceps femoris using a routine 8-mm punch biopsy device. All dogs were injected with butorphanol (0.2 mg/kg Vetorphale; Meiji Seika Pharm Co., Ltd., Tokyo, Japan) into the muscle for analgesia before waking from anesthesia. After the second CT scan (after 4 weeks of GC administration), the dogs were euthanized with an intravenous injection of sodium pentobarbital (100 mg/kg Nembutal; Abbott Japan, Tokyo, Japan), and a skeletal muscle sample was collected from the right biceps femoris with the 8-mm punch biopsy device.

Immunohistochemistry

To classify the fast-twitch and slow-twitch muscle fibers of the skeletal muscle, immunohistochemistry was performed using antibodies against the myosin heavy chain that is specifically expressed in fast-twitch and slow-twitch muscle fibers. All samples were embedded in paraffin and sliced into 3- μ m slices. The prepared slide sections were treated with 8,000-fold diluted primary antibody (M8421 and M4276; Sigma, St. Louis, MO, USA) at 4°C for 12-hr. Next, EnVision + System HRP Labeled Polymer Anti-Mouse IgG antibody (REF K4001; Dako, Santa Clara, CA, USA) was added to the sections as a secondary antibody, which was reacted at room temperature for 30 min. Color was developed using Liquid Dab + Substrate Chromogen System (Dako), and Mayer's hematoxylin was used as the counterstain. The cross-sectional area of the muscle fibers was measured using ImageJ software (National Institute of Health, Bethesda, MD, USA).

Real-time reverse transcription (RT)-polymerase chain reaction (PCR)

Total RNA was extracted from the skeletal muscle samples using SV Total System (Promega, Madison, WI, USA) and reverse-transcribed using ReverTra Dash (Toyobo Biochemicals, Osaka, Japan) according to the manufacturer's instructions. Primer sequences for 10 genes involved in the protein metabolism of humans and rodents, including Krüppel-like factor 15 (KLF15), forkhead box O1 (FOXO1), forkhead box O3 (FOXO3), muscle RING finger protein 1 (MuRF1), muscle atrophy F-box (Atrogin-1), growth factor receptor-bound protein 10 (GRB10), phosphotyrosine interaction domain-containing 1 (PID1), SH3 domain-containing 1 (SORBS1), p85 α subunit of phosphoinositide 3 kinase (p85 α), and Sestrin 1 (SESN1), are shown in Table 1. The sequence of the target gene was obtained from the Genbank database (<https://www.ncbi.nlm.nih.gov/genbank/>), and the optimum primer sequence was generated from the obtained sequence using Primer BLAST (<https://www.ncbi.nlm.nih.gov/tools/primer-blast/>). Based on the analyses of 10 samples amplified using primer sets for 8 genes (glyceraldehyde-3-phosphate dehydrogenase (GAPDH), β 2-microglobulin, hypoxanthine–guanine phosphoribosyltransferase, ribosomal protein L8, ribosomal protein L13, ribosomal protein S5, ribosomal protein S19, and succinate dehydrogenase) using BestKeeper software (<https://www.gene-quantification.de/bestkeeper.html>), we chose GAPDH as the housekeeping gene.

Quantitative PCR (qPCR) was performed using SYBR Premix Ex TaqII (Tli RNaseH Plus; TaKaRa Bio Inc., Kusatsu, Japan) on StepOnePlus™ Real-Time PCR System (Applied Biosystems, Foster City, CA, USA), and relative quantification was performed using the calibration curve method. PCR comprised an initial denaturation step at 95°C for 30 sec, followed by 40 cycles of amplification involving denaturation at 95°C for 15 sec and annealing and extension at 60°C for 30 sec. The specific amplification

Table 1. Primers for quantitative real-time RT-PCR

Gene		Sequence (5'-3')	GenBank accession number	Intra-assay coefficient of variation (%)
GAPDH	Forward	CACCAACTGCTTGGCTCCTC	AB038240.1	7.5
	Reverse	CGTCACGCCACATCTTCCCA		
KLF15	Forward	CAAGAGCAGCCACCTCAAG	XM_846268.4	15.3
	Reverse	GTCAAGCCCTACCACCTCAAG		
FoxO1	Forward	ACTTATGGCAGCCAGGCATC	XM_025462396.1	16.8
	Reverse	GCAAGGCACGCCATTAAC		
FoxO3	Forward	CCTTTAACAGCACGGTGTTCG	XM_003639400.4	11.7
	Reverse	GGTCCTGGAGTGTCTGGTTG		
MuRF1	Forward	CTGCAGAGCGTCTTCCAGG	XM_022413016.1	9.8
	Reverse	CTCCTTGGTCACTCGACAGG		
Atrogin1	Forward	TCATGCAGAGGCTGAGTGAC	XM_532324.6	9.7
	Reverse	GGATCTGCCGCTCAGAGAAG		
Grb10	Forward	CCACGGCTTCTGCATAAAGC	XM_014120815.2	7.9
	Reverse	CGTCATCCAGCACGTTTCTCC		
Pid1	Forward	CACCACAGGCATGCAGTTTC	XM_022409580.1	9.3
	Reverse	AGGTGATGGAGCCCACTTG		
Sorbs1	Forward	CATCCCGACAAGGCATCTTC	XM_014108803.2	9.1
	Reverse	CTTGCTGTGACTGGCAAAGT		
p85 α	Forward	ACCAGTACCGGAATGAGTCTC	XM_014108822.2	7.6
	Reverse	CCTCTTGACAACCTGATCCTG		
Sesn1	Forward	AAGTGTGTTTGCCTCCCG	XM_849248.5	7.8
	Reverse	GCTCTCAGAGCGTAGAGGAG		

of each gene was confirmed via agarose gel electrophoresis and melting curve analysis. qPCR was performed for all genes in a single plate. The intra-assay coefficient of variation value in qPCR quantification (n=8) was <20% (Table.1).

Statistical analyses

Excel 2004 (Microsoft, Redmond, WA, USA) with the add-in software Statcel 3 (OMS Publishing, Saitama, Japan) was used for statistical analyses. As some data were not normally distributed (Kolmogorov–Smirnov test), we employed the Wilcoxon signed-rank test for analyzing changes noted in the muscle cross-sectional area of the paraspinal muscle at L3 and the mid-femoral muscle using CT, muscle fiber cross-sectional area using immunohistochemistry, and mRNA expression levels using real-time RT-PCR before and after GC administration. *P* values <0.05 were considered significant.

RESULTS

Clinical signs and skeletal muscle cross-sectional area

All dogs showed polyuria/polydipsia after prednisolone administration for 4 weeks; however, none of the animals showed any other clinical signs, including the signs suggestive of muscle atrophy (such as lethargy or exercise intolerance). No gross muscle atrophy was observed in the physical examination. The results of the analyses of the skeletal muscle cross-sectional area of the paraspinal muscle at L3 and the mid-femoral muscle using CT are presented in Fig. 1. There was a significant reduction in the muscle cross-sectional area of the paraspinal muscle at L3 (from 27.5 ± 1.9 to 22.6 ± 2.0 cm², 17.6% decrease; *P*<0.05) and the mid-femoral muscle (from 55.1 ± 4.7 to 50.7 ± 4.1 cm², 9.3% decrease; *P*<0.05) after GC administration.

Muscle fiber cross-sectional area via immunohistochemistry

We investigated the cross-sectional area of fast-twitch and slow-twitch muscle fibers via immunohistochemistry. There were significant reductions in the cross-sectional areas of fast-twitch (from $2,779 \pm 369$ to $1,581 \pm 207$ μ m², 31.4% decrease; *P*<0.05) and slow-twitch (from $2,871 \pm 211$ to $1,971 \pm 169$ μ m², 43.2% decrease; *P*<0.05) muscle fibers (Fig. 2).

Relative RNA expression level before and after GC administration

Real-time RT-PCR was performed to compare changes in the expression level of 12 genes before and after GC administration. Relative *GRB10* expression was significantly increased after prednisolone administration (from 0.46 ± 0.089 to 1.0 ± 0.13 ; *P*<0.05). Although some dogs showed an increase in the expression of other genes after GC administration, no statistical significance was found (Fig. 3). *GRB10* showed less variation in its expression among the animals. By contrast, other genes exhibited large inter-individual variability, and the expression of these genes in some individuals was completely opposite to the expression of the same genes in others.

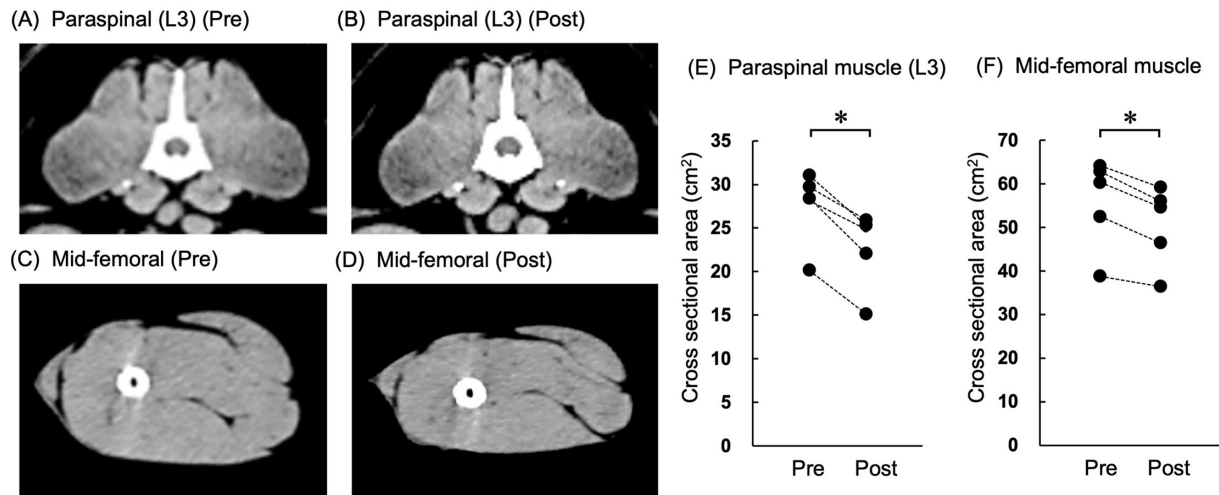


Fig. 1. Computed tomography images of the paraspinal muscle at L3 (A, B) and the mid-femoral muscle (C, D) and the cross-sectional area of the paraspinal muscle at L3 (E) and the mid-femoral muscle (F) before and after 4 weeks of prednisolone administration. Dot plot shows the cross-sectional area of the muscle before (Pre) and after (Post) prednisolone administration. *Significantly different ($P < 0.05$).

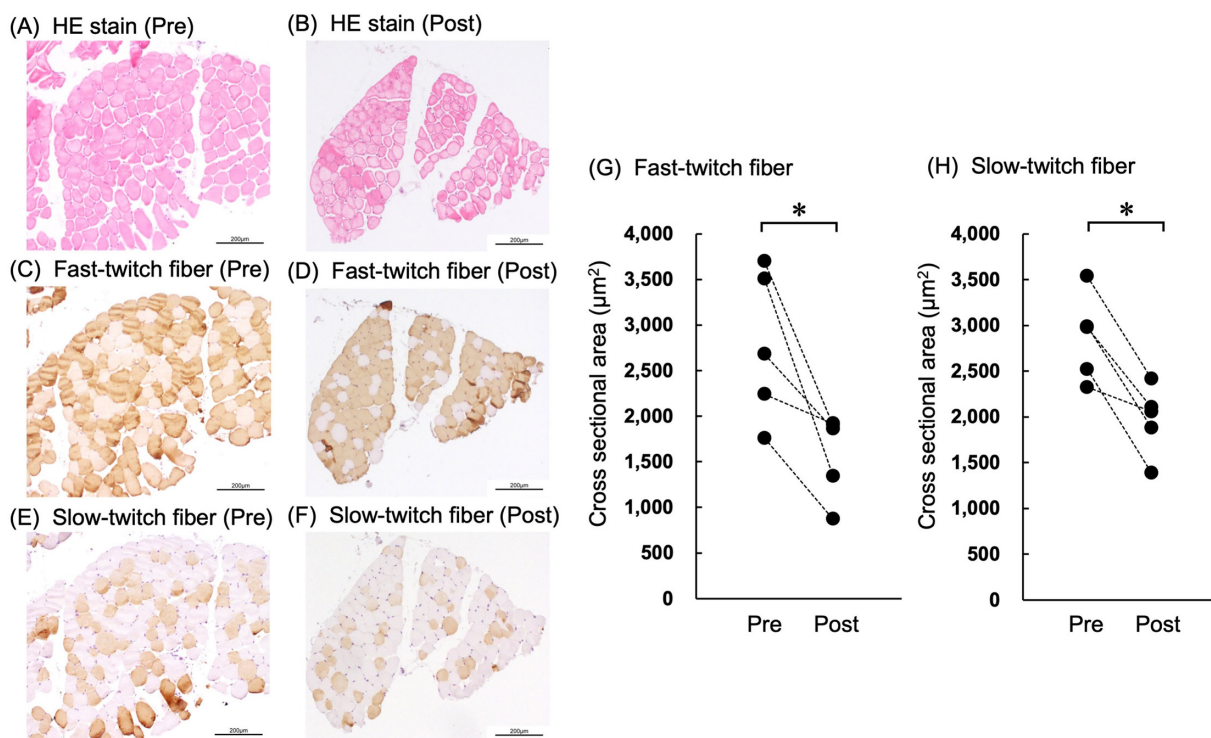


Fig. 2. Cross-section of fast- and slow-twitch muscle fibers before and after prednisolone administration. H&E stain before (A) and after (B) prednisolone administration, fast-twitch muscle fibers before (C) and after (D) prednisolone administration, and slow-twitch muscle fibers before (E) and after (F) prednisolone administration. The graphs are the dot plots of the fast-twitch (G) and slow-twitch (H) muscle fiber sectional area. Dot plot shows the cross-sectional area of the muscle fibers before (Pre) and after (Post) prednisolone administration. *Significantly different ($P < 0.05$).

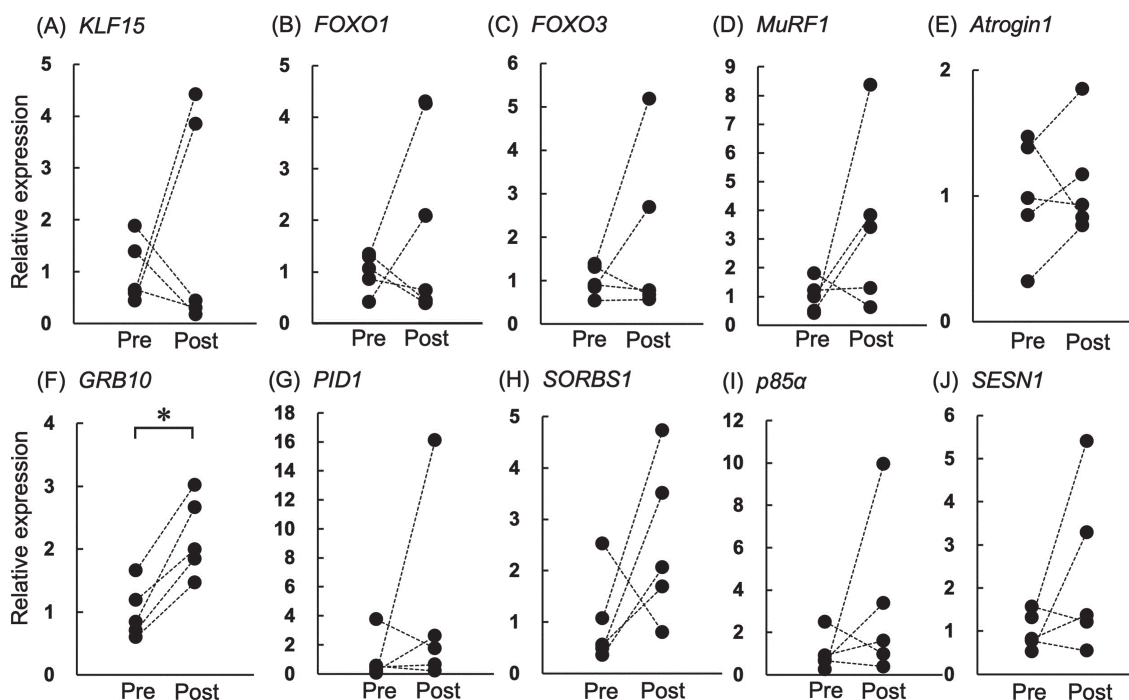


Fig. 3. Relative expression level of the skeletal muscle genes involved in protein metabolism before and after prednisolone administration. (A) *KLF15*, (B) *FOXO1*, (C) *FOXO3*, (D) *MuRF1*, (E) *Atrogin1*, (F) *GRB10*, (G) *PID1*, (H) *SORBS1*, (I) *p85α*, and (J) *SESN1*. *GAPDH* expression was used as the internal control. Dot plot shows the relative gene expressions before (Pre) and after (Post) prednisolone administration. *Significantly different ($P < 0.05$).

DISCUSSION

In the present study, we induced muscle atrophy using GC in dogs and investigated changes in gene expressions associated with muscle atrophy. First, we evaluated GC-induced muscle atrophy using CT. CT is considered the gold standard to measure muscle mass noninvasively [7] and has been applied for evaluating muscle atrophy caused by various diseases in humans [1, 36]. Several studies that evaluated human muscle atrophy via CT showed a significant loss of thigh, abdominal, and paraspinal muscle mass associated with exogenous or endogenous GCs [9, 14, 26]. In the present study, the cross-sectional area of the paraspinal muscle at L3 and the mid-femoral muscle was significantly reduced after GC administration in dogs. Although Braund *et al.* histologically evaluated GC-induced muscle atrophy in dogs [4], to the best of our knowledge, this is the first study that quantitatively investigated GC-induced muscle atrophy using CT in dogs. The results of the present study suggested that these two sites are useful for evaluating GC-induced muscle atrophy using CT in dogs. The present study showed that prednisolone administration at 1 mg/kg for 4 weeks in dogs led to marked muscle atrophy.

We then histologically evaluated muscle fibers before and after GC administration. Muscles are composed of two types of muscle fibers: fast- and slow-twitch muscle fibers. In our study, both fast- and slow-twitch muscle fibers were atrophied, and fast-twitch muscle fibers tended to show a severe decrease in the cross-sectional area. This is consistent with the findings of previous studies on humans and rodents that showed that fast-twitch muscle fibers were significantly atrophied after GC administration, whereas slow-twitch muscle fibers were less affected [8, 11, 29, 35]. Likewise, in a previous study on dogs, prednisolone administration at 4 mg/kg/day for 4 weeks resulted in predominant atrophy in the fast-twitch muscle fibers of the biceps femoris [4]. By contrast, dogs with naturally-occurring hyperadrenocorticism showed atrophy in both the fast- and slow-twitch muscle fibers of the biceps femoris, with pronounced atrophy in the fast-twitch muscle fibers [5]. The GC sensitivity of the muscle fiber type may depend on the type, dose, and duration of GC exposure [5, 6, 18, 22, 41]; these factors may have resulted in differences in the extent of muscle fiber atrophy among these studies. The present study suggested that prednisolone administration at 1 mg/kg/day for 4 weeks induces muscle fiber atrophy similar to that in dogs with hyperadrenocorticism.

We also investigated changes in gene expression in the biceps femoris muscles before and after GC administration. Of the 10 genes that were investigated, *GRB10* expression was significantly increased after GC administration for 4 weeks. This result was consistent with the findings of a previous study, in which dexamethasone was added to mouse C2C12 myotubes [15]. *GRB10* inhibits insulin signaling by inhibiting the insulin receptor substrate (IRS)/phosphoinositide 3 kinase (PI3K)/serine–threonine kinase (AKT) pathway located upstream of the mammalian target of rapamycin complex 1 (mTORC1) [34, 45, 47]. Moreover, *GRB10* phosphorylated by mTORC1 directly suppresses the mTORC1 activity [47]. The mTORC1 pathway plays a central role in protein anabolism in the skeletal muscle [16, 23, 38]. In the present study, increase in *GRB10* expression was observed concurrently with GC-induced muscle atrophy, and *GRB10* might be involved in the pathophysiology of muscle atrophy through

the suppression of insulin signaling and the subsequent mTORC1 activity. Hence, GRB10 may possess an important role in GC-induced muscle atrophy in dogs.

In this study, along with *GRB10*, we investigated several genes involved in protein metabolism. *SORBS1*, *PID1*, and *p85 α* affect the IRS/PI3K/AKT pathway and inhibit insulin signaling in addition to *GRB10* [20, 45, 48]. *SESNI* is known to inhibit mTORC1 and its activator [17]. Therefore, *SORBS1*, *PID1*, *p85 α* , and *SESNI* are the factors involved in protein anabolic mechanisms. By contrast, *FOXO1*, *FOXO3*, *KLF15*, *Atrogin-1*, and *MuRF1* are involved in protein catabolic mechanisms, including autophagy and the ubiquitin–proteasome system [3, 10, 31, 32, 35]. In the present study, the expression levels of these catabolic and anti-anabolic genes increased after GC administration in some dogs; however, large individual variations were observed. These variations appeared to be independent of age or sex (Supplementary Tables 1 and 2). In a past study conducted on mice, dexamethasone increased the expression of *Atrogin-1* and *MuRF1* after 3 days; however, the expression decreased afterward despite continuous dexamethasone administration [12]. In addition, another study reported that the expression of genes involved in protein catabolism was not increased in the skeletal muscle of human patients with Cushing's syndrome [30]. These study findings suggest that the expressions of the catabolic and anti-anabolic genes increase only in the early stage of GC muscle atrophy in some individuals. Further research to evaluate serial changes in gene expressions is warranted to investigate the early pathology of GC-induced muscle atrophy in dogs.

There are some limitations to our study. First, a limited number of dogs were used in our study that reduced the power to detect statistically significant differences. Second, owing to limited image resolution, we could not distinguish individual muscles on CT. A high-resolution CT might have clearly showed changes in the mass of each muscle as well as differences in GC sensitivity. This could have contributed to a greater understanding of the pathophysiology of GC-induced muscle atrophy.

In conclusion, GC-induced muscle atrophy was quantitatively evaluated in dogs. Both the fast-twitch and slow-twitch muscle fibers were atrophied after prednisolone administration at 1 mg/kg/day for 4 weeks. *GRB10* expression was increased after GC administration, and GRB10 might be involved in the pathology of GC-induced muscle atrophy in dogs. The GRB10/AKT/mTORC1 pathway possibly plays a central role in GC-induced muscle atrophy in canines.

CONFLICT OF INTEREST. The authors declare no conflict of interest in this study.

ACKNOWLEDGMENTS. This work was supported by JSPS KAKENHI Grant Number 17K08102.

REFERENCES

1. Amini, B., Boyle, S. P., Boutin, R. D. and Lenchik, L. 2019. Approaches to assessment of muscle mass and myosteatosis on computed tomography: A systematic review. *J. Gerontol. A Biol. Sci. Med. Sci.* **74**: 1671–1678. [Medline] [CrossRef]
2. Behrend, E. N. and Kempainen, R. J. 1997. Glucocorticoid therapy. Pharmacology, indications, and complications. *Vet. Clin. North Am. Small Anim. Pract.* **27**: 187–213. [Medline] [CrossRef]
3. Bodine, S. C., Latres, E., Baumhueter, S., Lai, V. K. M., Nunez, L., Clarke, B. A., Poueymirou, W. T., Panaro, F. J., Na, E., Dharmarajan, K., Pan, Z. Q., Valenzuela, D. M., DeChiara, T. M., Stitt, T. N., Yancopoulos, G. D. and Glass, D. J. 2001. Identification of ubiquitin ligases required for skeletal muscle atrophy. *Science* **294**: 1704–1708. [Medline] [CrossRef]
4. Braund, K. G. 1980. Experimental Investigation Myopathy of Glucocorticoid-Induced in the Dog. *Exp. Neurol.* **68**: 50–71. [Medline] [CrossRef]
5. Braund, K. G., Dillon, A. R., Mikeal, R. L. and August, J. R. 1980. Subclinical myopathy associated with hyperadrenocorticism in the dog. *Vet. Pathol.* **17**: 134–148. [Medline] [CrossRef]
6. Braunstein, P. W. Jr. and DeGirolami, U. 1981. Experimental corticosteroid myopathy. *Acta Neuropathol.* **55**: 167–172. [Medline] [CrossRef]
7. Cruz-Jentoft, A. J., Baeyens, J. P., Bauer, J. M., Boirie, Y., Cederholm, T., Landi, F., Martin, F. C., Michel, J. P., Rolland, Y., Schneider, S. M., Topinková, E., Vandewoude, M., Zamboni M., European Working Group on Sarcopenia in Older People 2010. Sarcopenia: European consensus on definition and diagnosis. *Age Ageing* **39**: 412–423. [Medline] [CrossRef]
8. Dekhuijzen, P. N. R., Gayan-Ramirez, G., Bisschop, A., De Bock, V., Dom, R. and Decramer, M. 1995. Corticosteroid treatment and nutritional deprivation cause a different pattern of atrophy in rat diaphragm. *J. Appl. Physiol. (1985)* **78**: 629–637. [Medline] [CrossRef]
9. Delivanis, D. A., Iñiguez-Ariza, N. M., Zeb, M. H., Moynagh, M. R., Takahashi, N., McKenzie, T. J., Thomas, M. A., Gogos, C., Young, W. F., Bancos, I. and Kyriazopoulou, V. 2018. Impact of hypercortisolism on skeletal muscle mass and adipose tissue mass in patients with adrenal adenomas. *Clin. Endocrinol. (Oxf.)* **88**: 209–216. [Medline] [CrossRef]
10. Fisch, S., Gray, S., Heymans, S., Haldar, S. M., Wang, B., Pfister, O., Cui, L., Kumar, A., Lin, Z., Sen-Banerjee, S., Das, H., Petersen, C. A., Mende, U., Burleigh, B. A., Zhu, Y., Pinto, Y. M., Liao, R. and Jain, M. K. 2007. Kruppel-like factor 15 is a regulator of cardiomyocyte hypertrophy. *Proc. Natl. Acad. Sci. USA* **104**: 7074–7079. [Medline] [CrossRef]
11. Fournier, M., Huang, Z. S., Li, H., Da, X., Cercek, B. and Lewis, M. I. 2003. Insulin-like growth factor I prevents corticosteroid-induced diaphragm muscle atrophy in emphysematous hamsters. *Am. J. Physiol. Regul. Integr. Comp. Physiol.* **285**: R34–R43. [Medline] [CrossRef]
12. Gunder, L. C., Harvey, I., Redd, J. R., Davis, C. S., Al-Tamimi, A., Brooks, S. V. and Bridges, D. 2020. Obesity promotes glucocorticoid-dependent muscle atrophy in male C57BL/6J mice. *Biomedicine* **8**: 1–13. [Medline] [CrossRef]
13. Harvey, C. M. D. 1964. The basophil adenomas of the pituitary body and their clinical manifestations (Pituitary Basophilism). *J. Neurosurg.* **21**: 318–347. [CrossRef]
14. Horber, F. F., Scheidegger, J. R., Grünig, B. E. and Frey, F. J. 1985. Thigh muscle mass and function in patients treated with glucocorticoids. *Eur. J. Clin. Invest.* **15**: 302–307. [Medline] [CrossRef]
15. Kuo, T., Lew, M. J., Mayba, O., Harris, C. A., Speed, T. P. and Wang, J. C. 2012. Genome-wide analysis of glucocorticoid receptor-binding sites in myotubes identifies gene networks modulating insulin signaling. *Proc. Natl. Acad. Sci. USA* **109**: 11160–11165. [Medline] [CrossRef]
16. Laplante, M. and Sabatini, D. M. 2012. mTOR signaling in growth control and disease. *Cell* **149**: 274–293. [Medline] [CrossRef]
17. Lee, J. H., Cho, U. S. and Karin, M. 2016. Sestrin regulation of TORC1: Is Sestrin a leucine sensor? *Sci. Signal.* **9**: re5. [Medline] [CrossRef]
18. Levin, O. S., Polunina, A. G., Demyanova, M. A. and Isaev, F. V. 2014. Steroid myopathy in patients with chronic respiratory diseases. *J. Neurol.*

- Sci.* **338**: 96–101. [Medline] [CrossRef]
19. Lindsay, J. R., Nansel, T., Baid, S., Gumowski, J. and Nieman, L. K. 2006. Long-term impaired quality of life in Cushing's syndrome despite initial improvement after surgical remission. *J. Clin. Endocrinol. Metab.* **91**: 447–453. [Medline] [CrossRef]
 20. Mauvais-Jarvis, F., Ueki, K., Fruman, D. A., Hirshman, M. F., Sakamoto, K., Goodyear, L. J., Iannacone, M., Accili, D., Cantley, L. C. and Kahn, C. R. 2002. Reduced expression of the murine p85 α subunit of phosphoinositide 3-kinase improves insulin signaling and ameliorates diabetes. *J. Clin. Invest.* **109**: 141–149. [Medline] [CrossRef]
 21. Menezes, L. G., Sobreira, C., Neder, L., Rodrigues-Júnior, A. L. and Martinez, J. A. 2007. Creatine supplementation attenuates corticosteroid-induced muscle wasting and impairment of exercise performance in rats. *J. Appl. Physiol. (1985)* **102**: 698–703. [Medline] [CrossRef]
 22. Minetto, M. A., Lanfranco, F., Motta, G., Allasia, S., Arvat, E. and D'Antona, G. 2011. Steroid myopathy: some unresolved issues. *J. Endocrinol. Invest.* **34**: 370–375. [Medline] [CrossRef]
 23. Mirzoev, T., Tyganov, S., Vilchinskaya, N., Lomonosova, Y. and Shenkman, B. 2016. Key markers of mTORC1-dependent and mTORC1-independent signaling pathways regulating protein synthesis in rat soleus muscle during early stages of hindlimb unloading. *Cell. Physiol. Biochem.* **39**: 1011–1020. [Medline] [CrossRef]
 24. Morgan, S. A., Hassan-Smith, Z. K., Doig, C. L., Sherlock, M., Stewart, P. M. and Lavery, G. G. 2016. Glucocorticoids and 11 β -HSD1 are major regulators of intramyocellular protein metabolism. *J. Endocrinol.* **229**: 277–286. [Medline] [CrossRef]
 25. Mourtzakis, M., Prado, C. M. M., Lieffers, J. R., Reiman, T., McCargar, L. J. and Baracos, V. E. 2008. A practical and precise approach to quantification of body composition in cancer patients using computed tomography images acquired during routine care. *Appl. Physiol. Nutr. Metab.* **33**: 997–1006. [Medline] [CrossRef]
 26. Nawata, T., Kubo, M., Nomura, T., Oishi, K., Shiragami, K., Ikegami, T., Okada, M., Kobayashi, S. and Yano, M. 2018. Change in muscle volume after steroid therapy in patients with myositis assessed using cross-sectional computed tomography. *BMC Musculoskelet. Disord.* **19**: 93. [Medline] [CrossRef]
 27. Patel, R., Williams-Dautovich, J. and Cummins, C. L. 2014. Minireview: new molecular mediators of glucocorticoid receptor activity in metabolic tissues. *Mol. Endocrinol.* **28**: 999–1011. [Medline] [CrossRef]
 28. Pellegrino, M. A., D'Antona, G., Bortolotto, S., Boschi, F., Pastoris, O., Bottinelli, R., Polla, B. and Reggiani, C. 2004. Clenbuterol antagonizes glucocorticoid-induced atrophy and fibre type transformation in mice. *Exp. Physiol.* **89**: 89–100. [Medline] [CrossRef]
 29. Pette, D. and Staron, R. S. 1997. Mammalian skeletal muscle fiber type transitions. *Int. Rev. Cytol.* **170**: 143–223. [Medline] [CrossRef]
 30. Rallièrè, C., Tauveron, I., Taillandier, D., Guy, L., Boiteux, J. P., Giraud, B., Attaix, D. and Thiéblot, P. 1997. Glucocorticoids do not regulate the expression of proteolytic genes in skeletal muscle from Cushing's syndrome patients. *J. Clin. Endocrinol. Metab.* **82**: 3161–3164. [Medline]
 31. Rodriguez, J., Vernus, B., Chelhi, I., Cassar-Malek, I., Gabillard, J. C., Hadj Sassi, A., Seiliez, I., Picard, B. and Bonniieu, A. 2014. Myostatin and the skeletal muscle atrophy and hypertrophy signaling pathways. *Cell. Mol. Life Sci.* **71**: 4361–4371. [Medline] [CrossRef]
 32. Sandri, M., Sandri, C., Gilbert, A., Skurk, C., Calabria, E., Picard, A., Walsh, K., Schiaffino, S., Lecker, S. H. and Goldberg, A. L. 2004. Foxo transcription factors induce the atrophy-related ubiquitin ligase atrogin-1 and cause skeletal muscle atrophy. *Cell* **117**: 399–412. [Medline] [CrossRef]
 33. Santos, A., Resmini, E., Martínez Momblán, M. A., Valassi, E., Martel, L. and Webb, S. M. 2019. Quality of life in patients with Cushing's disease. *Front. Endocrinol. (Lausanne)* **10**: 862. [Medline] [CrossRef]
 34. Sapolsky, R. M., Romero, L. M. and Munck, A. U. 2000. How do glucocorticoids influence stress responses? Integrating permissive, suppressive, stimulatory, and preparative actions. *Endocr. Rev.* **21**: 55–89. [Medline]
 35. Sato, A. Y., Richardson, D., Cregor, M., Davis, H. M., Au, E. D., McAndrews, K., Zimmers, T. A., Organ, J. M., Peacock, M., Plotkin, L. I. and Bellido, T. 2017. Glucocorticoids induce bone and muscle atrophy by tissue-specific mechanisms upstream of E3 ubiquitin ligases. *Endocrinology* **158**: 664–677. [Medline]
 36. Schakman, O., Gilson, H. and Thissen, J. P. 2008. Mechanisms of glucocorticoid-induced myopathy. *J. Endocrinol.* **197**: 1–10. [Medline] [CrossRef]
 37. Schakman, O., Kalista, S., Barbé, C., Loumaye, A. and Thissen, J. P. 2013. Glucocorticoid-induced skeletal muscle atrophy. *Int. J. Biochem. Cell Biol.* **45**: 2163–2172. [Medline] [CrossRef]
 38. Sengupta, S., Peterson, T. R. and Sabatini, D. M. 2010. Regulation of the mTOR complex 1 pathway by nutrients, growth factors, and stress. *Mol. Cell* **40**: 310–322. [Medline] [CrossRef]
 39. Shimizu, N., Yoshikawa, N., Ito, N., Maruyama, T., Suzuki, Y., Takeda, S., Nakae, J., Tagata, Y., Nishitani, S., Takehana, K., Sano, M., Fukuda, K., Suematsu, M., Morimoto, C. and Tanaka, H. 2011. Crosstalk between glucocorticoid receptor and nutritional sensor mTOR in skeletal muscle. *Cell Metab.* **13**: 170–182. [Medline] [CrossRef]
 40. Swinney, G. R., Foster, S. F., Church, D. B. and Malik, R. 1998. Myotonia associated with hyperadrenocorticism in two dogs. *Aust. Vet. J.* **76**: 722–724. [Medline] [CrossRef]
 41. Tice, L. W. and Engel, A. G. 1967. The effects of glucocorticoids on red and white muscles in the rat. *Am. J. Pathol.* **50**: 311–333. [Medline]
 42. van Aken, M. O., Pereira, A. M., Biermasz, N. R., van Thiel, S. W., Hoftijzer, H. C., Smit, J. W. A., Roelfsema, F., Lamberts, S. W. J. and Romijn, J. A. 2005. Quality of life in patients after long-term biochemical cure of Cushing's disease. *J. Clin. Endocrinol. Metab.* **90**: 3279–3286. [Medline] [CrossRef]
 43. Webb, S. M., Badia, X., Barahona, M. J., Colao, A., Strasburger, C. J., Tabarin, A., van Aken, M. O., Pivonello, R., Stalla, G., Lamberts, S. W. J. and Glusman, J. E. 2008. Evaluation of health-related quality of life in patients with Cushing's syndrome with a new questionnaire. *Eur. J. Endocrinol.* **158**: 623–630. [Medline] [CrossRef]
 44. Webb, S. M., Santos, A., Resmini, E., Martínez-Momblán, M. A., Martel, L. and Valassi, E. 2018. Quality of life in cushing's disease: a long term issue? *Ann. Endocrinol. (Paris)* **79**: 132–137. [Medline] [CrossRef]
 45. Wick, K. R., Werner, E. D., Langlais, P., Ramos, F. J., Dong, L. Q., Shoelson, S. E. and Liu, F. 2003. Grb10 inhibits insulin-stimulated insulin receptor substrate (IRS)-phosphatidylinositol 3-kinase/Akt signaling pathway by disrupting the association of IRS-1/IRS-2 with the insulin receptor. *J. Biol. Chem.* **278**: 8460–8467. [Medline] [CrossRef]
 46. Yamanaka, K., Okuda, M. and Mizuno, T. 2019. Functional characterization of canine wild type glucocorticoid receptor and an insertional mutation in a dog. *BMC Vet. Res.* **15**: 363. [Medline] [CrossRef]
 47. Yu, Y., Yoon, S. O., Poulogiannis, G., Yang, Q., Ma, X. M., Villén, J., Kubica, N., Hoffman, G. R., Cantley, L. C., Gygi, S. P. and Blenis, J. 2011. Phosphoproteomic analysis identifies Grb10 as an mTORC1 substrate that negatively regulates insulin signaling. *Science* **332**: 1322–1326. [Medline] [CrossRef]
 48. Zeng, X. Q., Zhang, C. M., Tong, M. L., Chi, X., Li, X. L., Ji, C. B., Zhang, R. and Guo, X. R. 2012. Knockdown of NYGGF4 increases glucose transport in C2C12 mice skeletal myocytes by activation IRS-1/PI3K/AKT insulin pathway. *J. Bioenerg. Biomembr.* **44**: 351–355. [Medline] [CrossRef]